Figure S1

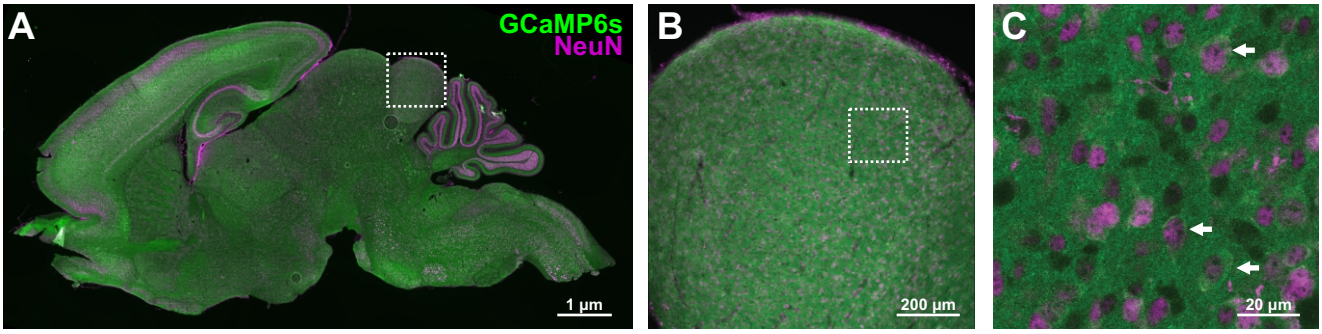

Figure S1. GCaMP6s expression in *Snap25-T2A-GCaMP6s* mice, related to Figure 1.

(A) Low magnification view of NeuN and GCaMP6s staining in a sagittal brain section taken from a P7 *Snap25-T2A-GCaMP6s* mouse. White square indicates area shown at higher magnification in B.

(B) High magnification view of NeuN and GCaMP6s immunostaining in the IC. White square indicates area shown at higher magnification in C.

(C) High magnification view of NeuN and GCaMP6s immunostaining in the IC.

Figure S2

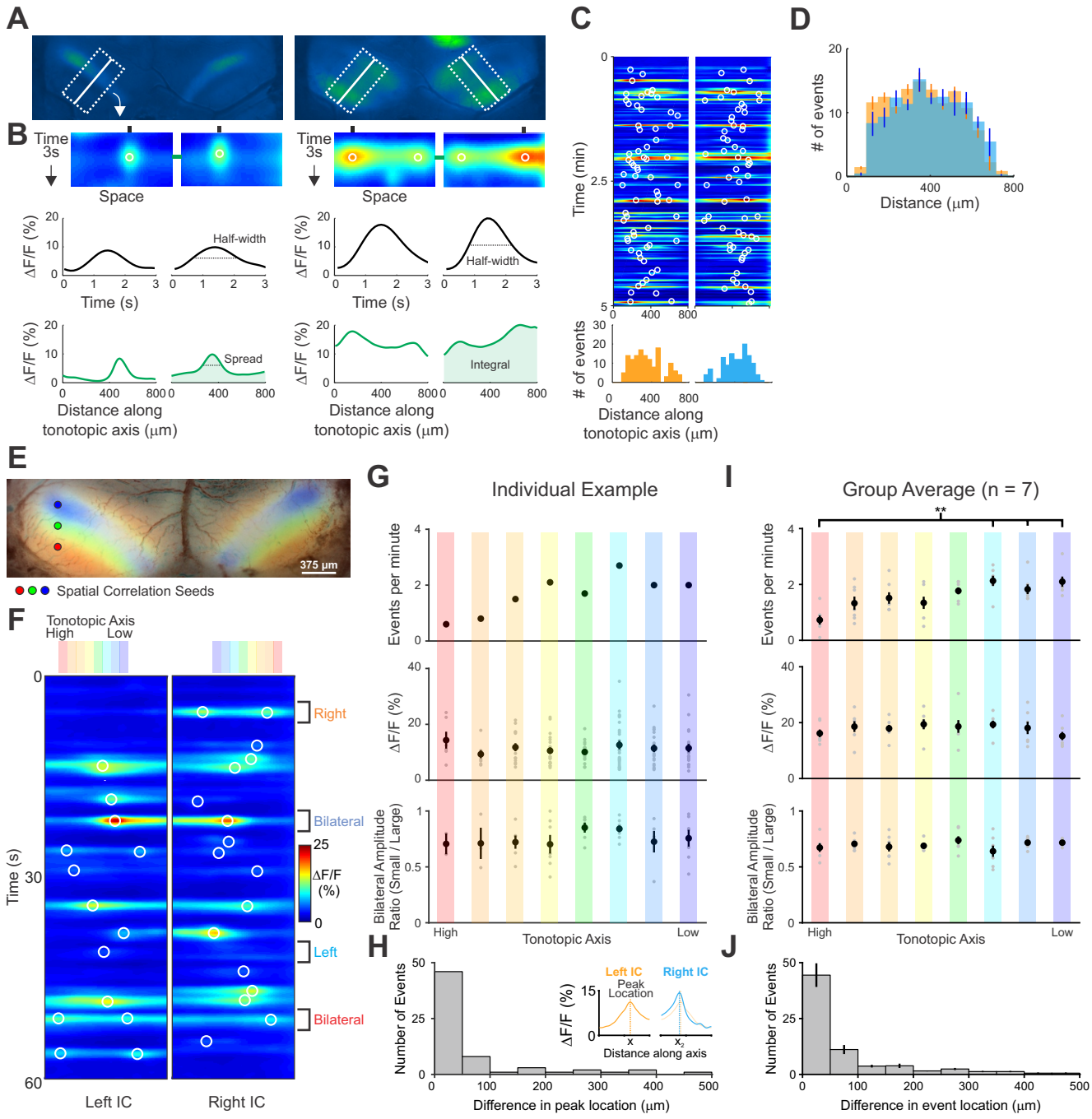
A
B
Time 3s
Space
ΔF/F (%)
Half-width
Time (s)
Spread
Integral
Distance along tonotopic axis (μm)
C
Time (min)
# of events
Distance along tonotopic axis (μm)
D
# of events
Distance (μm)
E
375 μm
Spatial Correlation Seeds
F
Tonotopic Axis
High
Low
Time (s)
Right
Bilateral
ΔF/F (%)
Left
Bilateral
Left IC
Right IC
G
Individual Example
Events per minute
ΔF/F (%)
Bilateral Amplitude Ratio (Small / Large)
High
Tonotopic Axis
Low
H
Number of Events
Left IC
Right IC
Peak Location
Distance along axis
Difference in peak location (μm)
I
Group Average (n = 7)
**
J
Difference in event location (μm)

Figure S2. Measurement of spatial location of events in the IC, related to Figure 1 and S5.

(A) Exemplars of a single-banded and double-banded event. Rectangular ROIs were placed as shown and averaged to create a 'line-scan' across the tonotopic axis.

(B) Monitoring fluorescence activity across space and time. Top: Heat maps of activity over time; circles indicate detected peaks. Middle: Change in fluorescence over time at the spatial location of the peak. Bottom: Change in florescence across the tonotopic axis at the time of the peak.

(C) Activity over a five-minute time frame in the left and right IC; circles indicate detected peaks. Bottom: histograms of peak locations.

(D) Histogram of average number of events across all control animals for left and right IC. n = 9 animals (two-way ANOVA, no comparisons reached statistical significance).

(E) Spatial correlation map generated from seeds across the tonotopic axis; high spatial and temporal correlation indicated by color (see Methods for details).

(F) Activity over a one-minute time frame in the left and right IC; circles indicate detected peaks. Activity was binned into 50 μm bins across the tonotopic axis as indicated by the colored bars above the plot.

(G) Exemplar plots of frequency, average amplitude, and average amplitude ratio of bilateral events examined across the tonotopic axis.

(H) Histogram of the difference in transient peak locations with bilaterally occurring events. Inset: Example of left and right peaks in space; the absolute value of the difference between these values is plotted.

(I) Plots of frequency, average amplitude, and average amplitude ratio of bilateral events examined across the tonotopic axis. n = 7 animals (one-way ANOVA, **: $P < 0.005$, all other comparisons: $P > 0.05$).

(J) Histogram of the difference in transient peak locations with bilaterally occurring events. n = 7 animals, error bars indicate S.E.M.

Figure S3

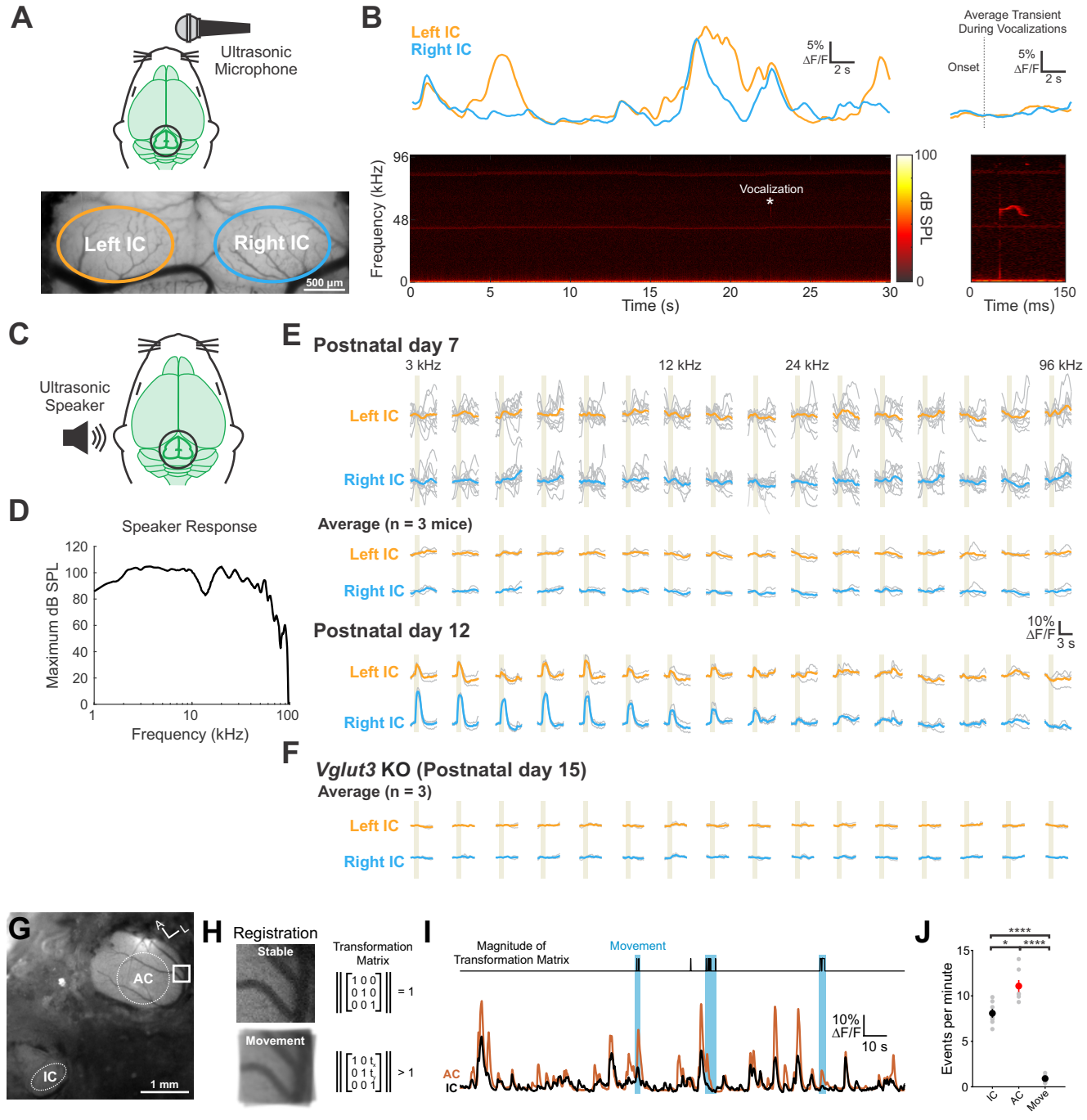
A
Ultrasonic Microphone
Left IC
Right IC
500 µm
B
Left IC
Right IC
5% ΔF/F
2 s
Average Transient During Vocalizations
Onset
Vocalization
Frequency (kHz)
96
48
0
dB SPL
100
0
Time (s)
Time (ms)
C
Ultrasonic Speaker
D
Speaker Response
Maximum dB SPL
Frequency (kHz)
E
Postnatal day 7
3 kHz
12 kHz
24 kHz
96 kHz
Average (n = 3 mice)
Postnatal day 12
10% ΔF/F
3 s
F
Vglut3 KO (Postnatal day 15)
Average (n = 3)
G
AC
IC
1 mm
H
Registration
Stable
Movement
Transformation Matrix
I
Magnitude of Transformation Matrix
Movement
10% ΔF/F
10 s
J
Events per minute
IC
AC
Move

Figure S3. Spontaneous events in the IC before hearing onset are not elicited by loud sounds or self-vocalization, related to Figure 1.

(A) Schematic depicting placement of ultrasonic microphone proximal to the mouth. ROIs were placed over the left and right IC as shown.

(B) Example transients (top) and concurrent spectrogram (bottom) during spontaneous activity. *: ultrasonic vocalization that is expanded on the right. Average transient during vocalizations taken across 5 animals.

(C) Schematic depicting placement of ultrasonic speaker placed next to the left ear (10 cm).

(D) Speaker response (at 0 dB attenuation) measured by the ultrasonic probe in dB sound pressure level (SPL) across all frequencies played.

(E) Transients concurrent with tones (1 s duration, sinusoidal amplitude modulation of 10Hz, beige bars) for P7 and P12 *Snap25-T2A-GCaMP6s* mice. Top panel represents an exemplar with grey traces representing individual trials and the colored lines indicating the mean. Large fluctuations are spontaneous events. Bottom panel represents an exemplar P12 mouse. Grey traces are individual tries and colored liens are the mean.

(F) Transients concurrent with tones played to P15 *Snap25-T2A-GCaMP6s*;*Vglut3*$^{-/-}$ mice.

(G) Simultaneous imaging of IC and AC before hearing onset. Box indicates area to be registered for movement detection.

(H) Frames registered for movement detection. If the animal moves, the magnitude of the transformation matrix required to correct the movement will increase.

(I) Plot of the magnitude of the transformation matrix and calcium transients in the IC and AC. Blue boxes indicate detected periods of movement.

(J) Plot of the frequency of calcium transients in the IC, AC, and movements during imaging. Grey circles are individuals, dark points are mean ± S.E.M.

Figure S4

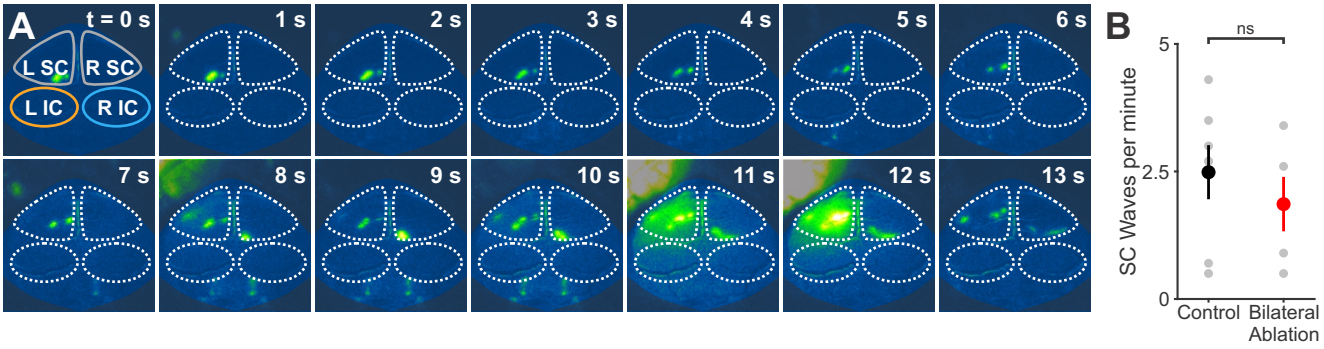

Figure S4. Retinal waves persist following bilateral cochlear ablation, related to Figure 3.
(A) Time series of calcium transients in the midbrain following bilateral cochlear ablation. Note the persistence of activity in both lobes of the superior colliculus and cortex.
(B) Plot of SC wave frequency in control and bilateral ablation experiments. n = 8 animals for control and n = 5 animals for bilateral ablation (two-tailed unpaired Student's t-test, ns: not significant).

Figure S5

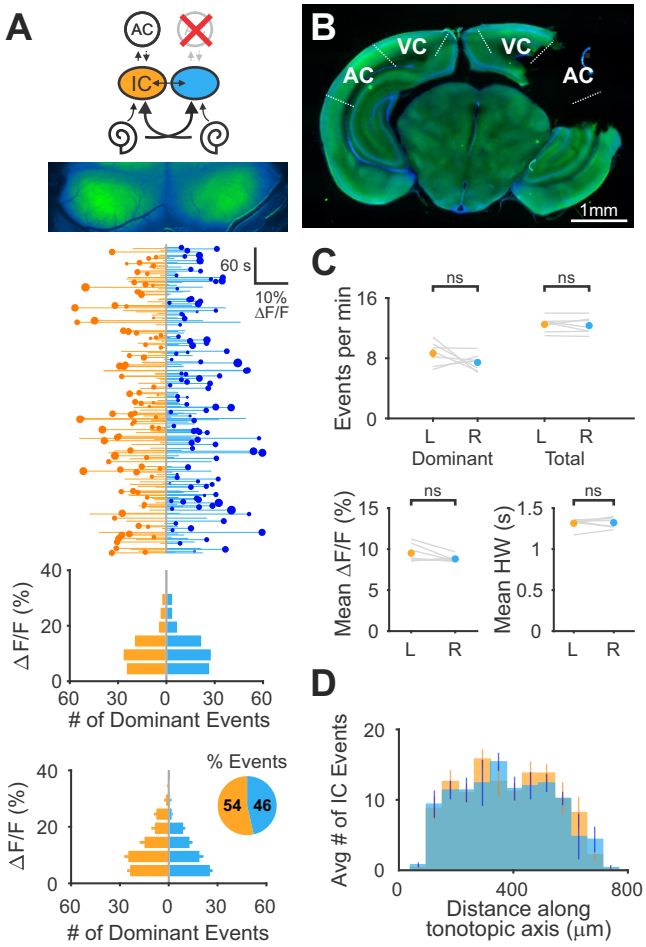

Figure S5. Spontaneous activity in the inferior colliculus is unaffected by auditory cortex ablation, related to Figure 4.

(A) Top: circuit diagram of auditory system with auditory cortex resected and average intensity image over the imaging session. Middle: Activity over time in left and right IC where each line indicates a detected event, the circle indicates the dominant lobe, and the size of the circle indicated the difference in fluorescence. Bottom: Histogram of the dominant events and histogram across the group.

(B) Coronal section of brain after auditory cortex resection.

(C) Comparison of event frequency, mean fluorescence change, and mean half-width of events in the left and right lobe of the IC. n = 7 animals (two-tailed paired Student's t-test with Bonferroni correction, ns: not significant).

(D) Distribution of event locations in left (orange) and right (blue) lobe of the IC (see Figure S2). n = 7 animals (two-way ANOVA, ns: not significant).

Figure S6

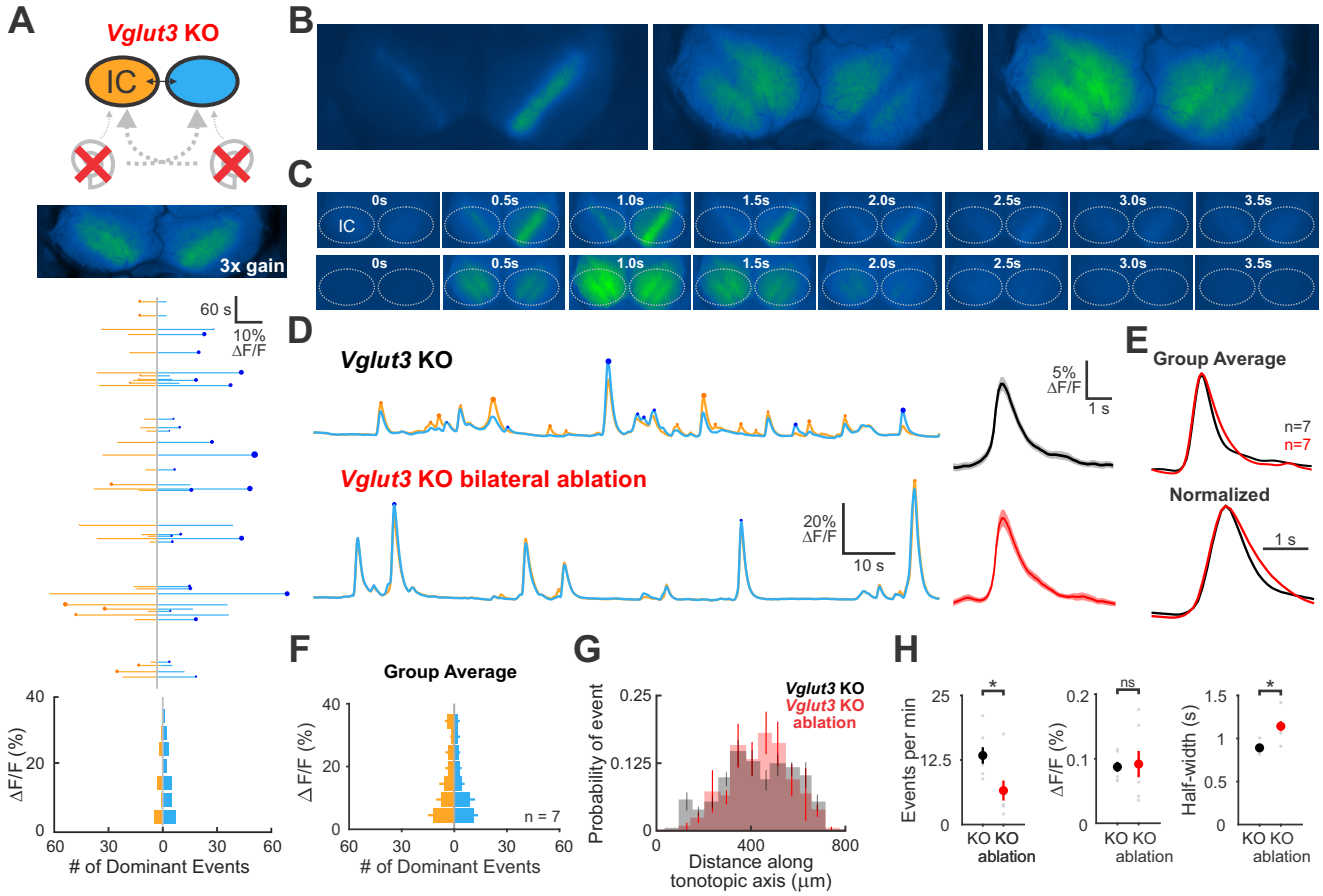

Figure S6. IC activity in *Vglut3* KO mice is dramatically reduced following bilateral cochlear ablation, related to Figure 5.

(A) Top: circuit diagram of auditory system, bilateral cochlear ablations were performed in *Snap25-T2A-GCaMP6s*;*Vglut3*$^{-/-}$ mice, and average intensity image over the 10-minute imaging session. Middle: Activity over time in left and right IC where each line indicates a detected event, the circle indicates the dominant lobe, and the size of the circle indicates the difference in fluorescence. Bottom: Histogram of the dominant events.

(B) Exemplar single- and double-banded events persist following bilateral ablation.

(C) Time-series of events observed following bilateral ablation.

(D) Example fluorescence transients from *Vglut3* KO and *Vglut3* KO mice following bilateral ablation. Right: Averages for events detected from trace to the left.

(E) Average and amplitude normalized transients from *Vglut3* KO and *Vglut3* KO mice following bilateral ablation.

(F) Group histogram across all animals (n = 7).

(G) Distribution of event locations in *Vglut3* KO (black) and *Vglut3* KO following bilateral ablation (red). n = 7 animals each (two-way ANOVA, ns: not significant).

(H) Comparisons of average frequency, amplitude, and half-width *Vglut3* KO and *Vglut3* KO mice following bilateral ablation. n = 7 animals each, (two-tailed unpaired Student's t-test with Bonferroni correction, ns: not significant, * P < 0.05).

Figure S7

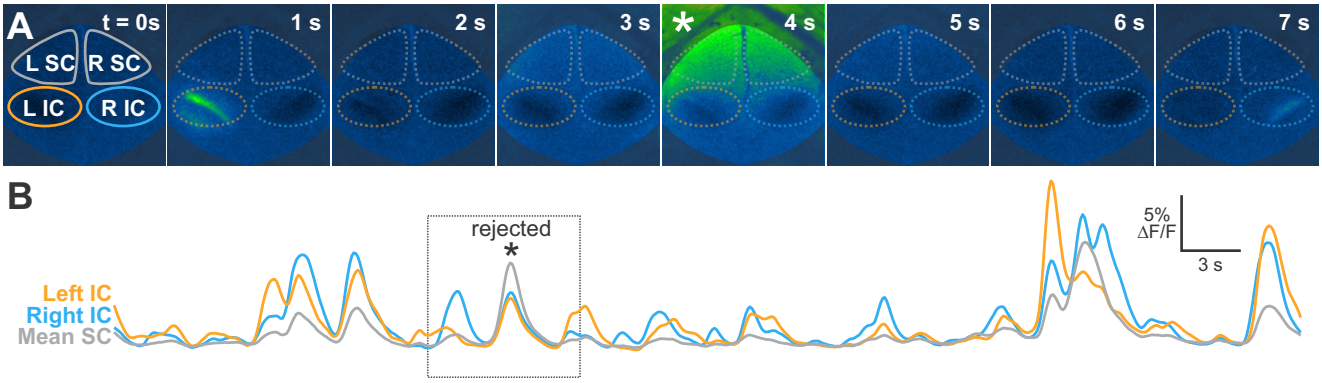

Figure S7. Large scale transients encompassing cortex and midbrain, related to Figure 1 and Methods.

(A) Time series of calcium transients in the midbrain. *: large scale transient observed across the entire midbrain. This activity is not spatially organized.

(B) Normalized fluorescence traces of the ROIs indicated in A, box indicates time series shown in A. When peaks in the SC displayed higher fluorescence changes than the IC, peaks in the IC were excluded from analysis.